

A&A manuscript no.  
(will be inserted by hand later)

Your thesaurus codes are:  
02(12.12.1; 11.03.1)

ASTRONOMY  
AND  
ASTROPHYSICS  
1.2.2018

# Structure formation: a spherical model for the evolution of the density distribution

P. Valageas

Service de Physique Théorique, CEA Saclay, 91191 Gif-sur-Yvette, France  
Theoretical Astrophysics Center, Juliane Maries Vej 30, 2100 Copenhagen 0, Denmark

Received November 25, 1997; accepted May 12, 1998.

**Abstract.** Within the framework of hierarchical clustering we show that a simple Press-Schechter-like approximation, based on spherical dynamics, provides a good estimate of the evolution of the density field in the quasi-linear regime up to  $\Sigma \sim 1$ . Moreover, it allows one to recover the exact series of the cumulants of the probability distribution of the density contrast in the limit  $\Sigma \rightarrow 0$  which sheds some light on the rigorous result and on “filtering”. We also obtain similar results for the divergence of the velocity field.

Next, we extend this prescription to the highly non-linear regime, using a stable-clustering approximation. Then we recover a specific scaling of the counts-in-cells which is indeed seen in numerical simulations, over a well-defined range. To this order we also introduce an explicit treatment of the behaviour of underdensities, which takes care of the normalization and is linked to the low-density bubbles and the walls one can see in numerical simulations. We compare this to a 1-dimensional adhesion model, and we present the consequences of our prescription for the power-law tail and the cutoff of the density distribution.

form broader and broader halos as larger scales become non-linear. These halos will produce galaxies or clusters of galaxies, according to the scale and other physical constraints like cooling processes. Hence it is of great interest to understand the evolution with time of the density field and the mass functions of various astrophysical objects it implies. This is a necessary step in order to model for instance the formation of galaxies or clusters, which can later put constraints on the cosmological parameters using the observed luminosity function of galaxies or the QSO absorption lines.

Within this hierarchical framework an analytical model for the mass function of collapsed (or just-virialized) objects was proposed by Press & Schechter (1974) (hereafter PS). Numerical simulations (Efstathiou et al.1988; Kauffmann & White 1993) have shown this mass function is similar to the numerical results, although the agreement is improved by a modification of the usual density threshold  $\delta_c$  used in this model (Lacey & Cole 1994). However, this prescription encounters some serious defects, like the cloud-in-cloud problem studied by Bond et al.(1991), and a well-known normalization problem since one only counts half of the mass of the universe. Moreover, underdense regions are not modelled by this approach, and are simply taken into account in fine by a global multiplication of the mass function by a factor 2 which allows to get the correct normalization (this multiplicative factor 2 was recovered more rigorously by Bond et al.1991 for a top-hat in  $k$ , but this does not extend to more realistic filters). Finally, this model only predicts the mass function of collapsed objects, while one may also be interested in mass condensations of various density, in order to study galaxies or even underdense structures (“voids”) for instance.

A method to describe the density field itself, and then derive the multiplicity functions of any objects, is to consider the counts-in-cells. These are closely related to the many-body correlation functions and were studied in detail by Balian & Schaeffer (1989) in the highly non-linear

---

**Key words:** cosmology: large-scale structure of Universe  
- galaxies : clustering

## 1. Introduction

In the standard cosmological model gravitational structures in the universe have formed by the growth of small density fluctuations present in the early universe (Peebles 1980). These perturbations may be due to quantum mechanical effects and are likely to be gaussian, so that they are described by their power-spectrum. In many cases, like the CDM model (Peebles 1982; Davis et al.1985), the power increases at small scales which leads to a hierarchical scenario of structure formation. Small scales collapse first, building small virialized objects which merge later to

regime within the framework of the stable clustering picture (Peebles 1980), where the correlation functions are scale-invariant. This assumption and the scaling it implies for the matter distribution are indeed verified by numerical simulations (Bouchet et al.1991; Colombi et al.1995) and observations (Maurogordato et al.1992). Bernardeau & Schaeffer (1991) and Valageas & Schaeffer (1997) (hereafter VS) described some of the consequences of this model for the multiplicity functions of various objects like clusters or galaxies. Indeed, a great advantage of this approach is that one can study many different astrophysical objects (and even “voids”) from a unique model which is not restricted to just-collapsed objects. Moreover, it is based on a rather general assumption, which does not depend on the exact details of the dynamics, and VS showed that the PS prescription can be recovered as a particular case among the possible models this scale-invariant approach can describe. Note that since the PS approach is unlikely to give a very precise description of the clustering process, because of its simplicity and the problems it encounters, the scale-invariant method offers the advantage to provide a simple and natural way to take into account the possible corrections to the PS prescription.

In this article, we intend to show how a simple PS-like model, based on the spherical dynamics, can describe the evolution of the density field and provide a specific model for the scale-invariant picture studied in Balian & Schaeffer (1989) or VS. Thus, we consider both the quasi-linear ( $\Sigma < 1$ ) and highly non-linear ( $\Sigma \gg 1$ ) regimes (where as usual  $\Sigma(M, a)$  is the amplitude of the density fluctuations at scale  $M$  given by the linear theory at the considered time), to relate the final non-linear density field to the initial conditions and to show how the scale-invariance of the many-body correlation functions and the scalings of the multiplicity functions described in VS can arise from the hierarchical structure formation scenario. We focus on the counts-in-cells, which provide a powerful description of the density field and can be used to obtain any mass function of interest as detailed in VS. First, we derive the statistics of the counts-in-cells which our spherical model implies in the quasi-linear regime (Sect.2). We show in particular that we recover in the limit  $\Sigma \rightarrow 0$  the whole series of the cumulants derived rigorously by Bernardeau (1994a) from the exact equations of motion. We also consider the predictions of this model for the statistics of the divergence of the velocity field (Sect.3) and explain why this simple spherical dynamics works so well in the limit  $\Sigma \rightarrow 0$  (Sect.4). Finally, we study the non-linear regime (Sect.5). In addition to the virialization process of overdensities we take care explicitly of the evolution of underdensities. This new prescription solves in a natural way the normalization problem (in the sense that all the mass will eventually get embedded within overdense halos) and is compared with a 1-dimensional adhesion model. It also allows to complete the comparison with the scale-invariant approach. Indeed, although we do not obtain as detailed

results for the mass function as the PS approach, which we believe anyway to be rather illusory since such simple and crude descriptions cannot provide rigorous and exact predictions, we think our model allows to understand how scaling properties appear, and it can predict asymptotic behaviours like the slope of the power-law tail of the mass function or its exponential cutoff (so that the model can be tested). Moreover, it gives a useful reference which would enable one to evaluate the magnitude of the effects neglected here from a comparison with the results obtained by a more rigorous calculation.

## 2. Quasi-linear regime: density contrast

As VS showed, it is possible to extend the usual PS approach to obtain an approximation of the density field and the counts-in-cells it implies, in addition to the mass function of just-virialized objects one generally considers. Although VS focused on the highly non-linear regime (using the stable-clustering ansatz), we shall here first consider the simpler case of the quasi-linear regime  $\Sigma < 1$ .

### 2.1. Critical universe: $\Omega = 1$

#### 2.1.1. Lagrangian point of view

We first consider a Lagrangian point of view, which is well suited to PS-like approaches since the fundamental hypothesis of such approximations is that it is possible to follow the evolution of fluid elements recognized in the early linear universe (one usually only considers overdensities) up to the non-linear regime. Thus, the usual PS prescription assumes i) that the dynamics of these objects is given by the spherical model and ii) that they keep their identity throughout their evolution. Hence, to any piece of matter identified in the early linear universe one can assign at a later time a specified radius and density. Of course, this cannot be exact as all particles cannot follow simultaneously a spherical dynamics, and this approach cannot take into account mergings which change the number of objects and destroy their identity. However, we shall see below that it can provide a reasonable estimate of the early density field.

In this Lagrangian approach, we consider the evolution of “objects” of mass  $M$ , identified in the early linear universe. In other words, the filtering scale is the mass and not the radius. According to the spherical model, particles which were initially embedded in a spherical region of space characterized by the density contrast  $\delta_L$  ( $\delta_L$  is the density contrast given by the linear theory at any considered time:  $\delta_L \propto a$  where  $a(t)$  is the scale factor) find themselves in a spherical region of density contrast  $\delta$  at the same scale  $M$ , given at any epoch by:

$$\delta = \mathcal{F}(\delta_L) \quad (1)$$

The function  $\mathcal{F}$  is defined by the dynamics of the spherical model (Peebles 1980):

$$\delta_L > 0 : \begin{cases} 1 + \delta = \frac{9}{2} \frac{(\theta - \sin \theta)^2}{(1 - \cos \theta)^3} \\ \delta_L = \frac{3}{20} [6(\theta - \sin \theta)]^{2/3} \end{cases} \quad (2)$$

and

$$\delta_L < 0 : \begin{cases} 1 + \delta = \frac{9}{2} \frac{(\sinh \eta - \eta)^2}{(\cosh \eta - 1)^3} \\ \delta_L = -\frac{3}{20} [6(\sinh \eta - \eta)]^{2/3} \end{cases} \quad (3)$$

This definition of  $\mathcal{F}(\delta_L)$  breaks down for  $\delta_L \geq \delta_c$ , with  $\delta_c = 3/20 (12\pi)^{2/3} \simeq 1.69$ , where  $\delta$  becomes infinite. This is usually cured by a virialization prescription: the halo is assumed to virialize in a finite radius taken for instance as one half its radius of maximum expansion, so that  $\mathcal{F}(\delta_c) = \Delta_c$  with  $1 + \Delta_c = 18\pi^2 \simeq 178$ . However, we shall not consider this modification in this section, as we focus here on the quasi-linear regime where most of the mass is embedded within regions of space with a density contrast  $\delta$  smaller than  $\Delta_c$ , hence we restrict ourselves to  $\delta < \Delta_c$ . Now, we define the Lagrangian probability distribution  $P_m(\delta)$ : if we choose at random a spherical region of mass  $M$  its density contrast is between  $\delta$  and  $\delta + d\delta$  with probability  $P_m(\delta) d\delta$  (here the index  $m$  does not stand for a given mass scale, its use is only to distinguish the Lagrangian quantities used here, where we follow matter elements, from their Eulerian counterparts which we shall introduce in the next sections). Within the framework of the spherical model, this probability distribution is simply given by:

$$P_m(\delta) d\delta = P_L(\delta_L) d\delta_L \quad \text{with} \quad \delta = \mathcal{F}(\delta_L) \quad (4)$$

where  $P_L(\delta_L)$  is the probability distribution relative to the linear density contrast, or the early universe. We shall assume that the initial density fluctuations are gaussian, so that:

$$P_L(\delta_L) = \frac{1}{\sqrt{2\pi}\Sigma} e^{-\delta_L^2/(2\Sigma^2)} \quad (5)$$

where as usual  $\Sigma = \Sigma(M, a)$  is the amplitude of the density fluctuations at scale  $M$  given by the linear theory at the considered time ( $\Sigma \propto a M^{-(n+3)/6}$  for an initial power-spectrum which is a power-law:  $P(k) \propto k^n$ ). We can note that the probability distribution  $P_m(\delta)$  is correctly normalized:  $\int P_m(\delta) d\delta = 1$  by definition. However, the mean value of  $\delta$  is not equal to 0. This is quite natural since particles get embedded within increasingly high overdensities (while the density contrast cannot be smaller than  $-1$ ), and at late times one expects that all the mass will be part of overdense virialized halos. However, this

late stage is not described by the model introduced in this section, which does not include virialization and where half of the mass remains at any time within underdensities (this is the well-known normalization problem of the PS prescription by a factor 2).

We can also characterize the probability distribution  $P_m(\delta)$  by the generating function  $\varphi_m(y, \bar{\xi}_m)$  (and by  $\bar{\xi}_m$ ) which we define by:

$$e^{-\varphi_m(y, \bar{\xi}_m)/\bar{\xi}_m} = \int_{-1}^{\infty} e^{-\delta y/\bar{\xi}_m} P_m(\delta) d\delta \quad (6)$$

where  $\bar{\xi}_m = \langle \delta^2 \rangle$ . The function  $\varphi_m(y, \bar{\xi}_m)$  generates the series of the moments of  $P_m(\delta)$ :

$$e^{-\varphi_m(y, \bar{\xi}_m)/\bar{\xi}_m} = 1 + \sum_{p=1}^{\infty} \frac{(-1)^p}{p!} y^p \frac{\langle \delta^p \rangle}{\bar{\xi}_m^p} \quad (7)$$

In the highly non-linear regime considered by VS the function  $\varphi_m(y, \bar{\xi}_m)$  was assumed to be scale-invariant, so that it did not depend on  $\bar{\xi}_m$ , but here this is not the case. If  $\langle \delta \rangle = 0$  the usual series of the cumulants is generated by  $\varphi(y, \bar{\xi}_m)$ :

$$\langle \delta \rangle = 0 : \varphi_m(y, \bar{\xi}_m) = \sum_{p=2}^{\infty} \frac{(-1)^{p-1}}{p!} y^p \frac{\langle \delta^p \rangle_c}{\bar{\xi}_m^{p-1}} \quad (8)$$

The relation (6) can be written in terms of the linear density contrast  $\delta_L$ :

$$e^{-\varphi_m(y, \bar{\xi}_m)/\bar{\xi}_m} = \int_{-\infty}^{\infty} \frac{d\delta_L}{\sqrt{2\pi}\Sigma} \times \exp \left[ -\frac{1}{\Sigma^2} \left( \frac{\delta_L^2}{2} + \mathcal{F}(\delta_L) y \frac{\Sigma^2}{\bar{\xi}_m} \right) \right] \quad (9)$$

In the quasi-linear regime, that is for  $\bar{\xi}_m \rightarrow 0$ ,  $\Sigma \rightarrow 0$  and  $\Sigma^2/\bar{\xi}_m \rightarrow 1$ , we can use the saddle point method to get:

$$\begin{cases} \varphi_m(y) = y \mathcal{F}(\delta_y) + \delta_y^2/2 \\ \delta_y = -y \mathcal{F}'(\delta_y) \end{cases} \quad (10)$$

where  $\varphi_m(y)$  is the limit of  $\varphi_m(y, \bar{\xi}_m)$  for  $\bar{\xi}_m \rightarrow 0$ . If we define  $\tau_m = -\delta_y$  and  $\mathcal{G}_m(\tau_m) = \mathcal{F}(\delta_y)$ , we obtain

$$\begin{cases} \varphi_m(y) = y \mathcal{G}_m(\tau_m) - y \tau_m \mathcal{G}'_m(\tau_m)/2 \\ \tau_m = -y \mathcal{G}'_m(\tau_m) \end{cases} \quad (11)$$

This is exactly the result derived rigorously by Bernardeau (1994a) from the equations of motion, when the matter is described by a pressure-less fluid. Hence our approach should give a good description of the early stages of gravitational clustering, since it leads to the right limit for the cumulants in the linear regime, which was not obvious at first sight. Moreover, it provides some hindsight into

the result of the exact calculation, as the function  $\mathcal{F}$  or  $\mathcal{G}_m$  which represents the spherical dynamics appears naturally in the expression of  $\varphi_m(y)$ . We shall come back to this point in Sect.4. We can note that our model implies in addition a specific dependence of  $\varphi_m(y, \bar{\xi}_m)$  on  $\bar{\xi}_m$  (or  $\Sigma$ ), which could be computed from (9).

### 2.1.2. Eulerian point of view

For practical purposes, one is in fact more interested in the Eulerian properties of the density field, where the filtering scale is a length scale  $R$ . For instance, a convenient way to describe the density fluctuations is to consider the counts-in-cells: one divides the universe into cells of scale  $R$  (and volume  $V$ ) and defines the probability distribution  $P(\delta)$  of the density contrast within these cells. Hence, we need to relate this Eulerian description to the Lagrangian model we developed in the previous section. As was done in VS, we shall use:

$$\int_{\delta}^{\infty} (1 + \delta') P(\delta') d\delta' = F_m(> \delta, M) \quad (12)$$

with  $M = (1 + \delta) \bar{\rho} V$ . Thus the mass embedded in cells of scale  $R$  with a density contrast larger than  $\delta$  is taken equal to the mass formed by particles which are located within spherical regions of scale  $M$  with a density contrast larger than  $\delta$ . Using our Lagrangian model, we get:

$$F_m(> \delta, M) = F_{mL}(> \delta_L, M) \quad \text{with} \quad \delta = \mathcal{F}(\delta_L) \quad (13)$$

where  $F_{mL}$  is the mass fraction obtained in the linearly extrapolated universe. From (12) and (5) we have:

$$(1 + \delta) P(\delta) = - \frac{\partial}{\partial \delta} \int_{\delta_L/\Sigma(R_m)}^{\infty} e^{-\nu^2/2} \frac{d\nu}{\sqrt{2\pi}} \quad (14)$$

with:

$$\begin{cases} \delta = \mathcal{F}[\delta_L] \\ R_m^3 = (1 + \delta) R^3 \end{cases} \quad (15)$$

Finally, we obtain:

$$P(\delta) = \frac{1}{\sqrt{2\pi}} \frac{1}{1 + \delta} \frac{\partial}{\partial \delta} \left[ \frac{\delta_L}{\Sigma(R_m)} \right] \exp \left[ -\frac{1}{2} \left( \frac{\delta_L}{\Sigma} \right)^2 \right] \quad (16)$$

as in VS. Of course we recover all the mass of the universe  $\int (1 + \delta) P(\delta) d\delta = 1$ . In fact, half of the mass is in overdensities and the other half in underdensities, as was the case in the Lagrangian description. However, in general this probability distribution is not correctly normalized:  $\int P(\delta) d\delta \neq 1$  (but in the linear regime,  $\bar{\xi} \rightarrow 0$  and  $\Sigma \rightarrow 0$ , its normalization tends to unity).

We can still define a generating function  $\varphi(y, \bar{\xi})$ , as in (6), which leads to:

$$e^{-\varphi(y, \bar{\xi})/\bar{\xi}} = \int_{-1}^{\infty} \frac{d\delta}{\sqrt{2\pi}} \frac{1}{1 + \delta} \frac{\partial}{\partial \delta} \left[ \frac{\delta_L}{\Sigma(R_m)} \right] \times \exp \left[ -\frac{1}{\bar{\xi}} \left( \delta y + \frac{\delta_L^2}{2} \frac{\bar{\xi}}{\Sigma^2} \right) \right] \quad (17)$$

Using  $\delta = \mathcal{F}(\delta_L) = \mathcal{G}_m(\tau_m)$ , with  $\tau_m = -\delta_L$ , we define:

$$\begin{cases} \mathcal{G}(\tau) = \mathcal{G}_m \left( \tau \frac{\Sigma [(1 + \mathcal{G}(\tau))^{1/3} R]}{\sqrt{\bar{\xi}}} \right) \\ \tau(\delta) = \frac{\tau_m \sqrt{\bar{\xi}}}{\Sigma [(1 + \mathcal{G}(\tau))^{1/3} R]} \end{cases} \quad (18)$$

Hence  $\mathcal{G}_m(\tau_m) = \mathcal{G}(\tau) = \delta$ . In the quasi-linear regime, that is for  $\bar{\xi} \rightarrow 0$ ,  $\Sigma \rightarrow 0$  and  $\Sigma^2/\bar{\xi} \rightarrow 1$ , the saddle point method leads to:

$$\begin{cases} \varphi(y) = y \mathcal{G}(\tau) - y \tau \mathcal{G}'(\tau)/2 \\ \tau = -y \mathcal{G}'(\tau) \end{cases} \quad (19)$$

where  $\varphi(y)$  is the limit of  $\varphi(y, \bar{\xi})$  for  $\bar{\xi} \rightarrow 0$ . Thus, once again we recover the result derived rigorously by Bernardeau (1994a). Note that we should have modified  $P(\delta)$  in (17) since it is not correctly normalized, however if this modification only consists of a multiplication factor (which must go to unity in the limit  $\bar{\xi} \rightarrow 0$ ) and a change of the shape of  $P(\delta)$  for density contrasts much larger than  $\bar{\xi}$  as  $\bar{\xi} \rightarrow 0$ , this does not modify the function  $\varphi(y)$  we obtained. If the power-spectrum is a power-law  $P(k) \propto k^n$ , (16) can be written:

$$P(\delta) = \frac{(1 + \delta)^{(n-3)/6}}{\sqrt{2\pi}\Sigma(R)} \left[ \frac{1}{\mathcal{F}'(\delta_L)} + \frac{3 + n}{6} \frac{\delta_L}{1 + \delta} \right] \times \exp \left[ -\frac{1}{2} \left( \frac{\delta_L}{\Sigma(R)} (1 + \delta)^{(3+n)/6} \right)^2 \right] \quad (20)$$

If the power-spectrum is not a power-law, our method is still valid and we have to use (16). However, for a very smooth  $P(k)$ , like a CDM power-spectrum, an easier and still reasonable approximation is to use (20) where  $n$  is the local slope of the power-spectrum at scale  $R$ . We shall compare this approximation to numerical results in Sect.2.3. The fact that we recover the exact generating function  $\varphi(y, \bar{\xi})$  for  $\bar{\xi} \rightarrow 0$  suggests again that our prescription could provide reasonable results in the early linear universe when  $\bar{\xi} < 1$ . We shall see below that it is indeed the case, by a comparison with numerical simulations. We can note that our probability distributions (20) look rather different from those obtained by Bernardeau (1994a) since the high-density cutoff is usually different

from a simple exponential. However, they both agree with numerical results for  $\delta \ll \Delta_c$ . In fact, neither of these approaches should be used for large density contrasts  $\delta > \Delta_c$  where shell-crossing and virialization play an important role.

## 2.2. Open universe: $\Omega < 1$ , $\Lambda = 0$

### 2.2.1. Lagrangian point of view

In the case of an open universe, we can still apply the method described previously for a critical universe but there is now an additional time dependence in the relation  $\delta_L - \delta$ . Thus, (4) becomes:

$$P_m(\delta) d\delta = P_L(\delta_L) d\delta_L \quad \text{with} \quad \delta = \mathcal{F}(\delta_L, a) \quad (21)$$

In the specific case where  $\Lambda = 0$ , one defines:

$$\eta_b = \cosh^{-1} \left( \frac{2}{\Omega} - 1 \right) \quad (22)$$

and

$$D(t) = \frac{3 \sinh \eta_b (\sinh \eta_b - \eta_b)}{(\cosh \eta_b - 1)^2} - 2 \quad (23)$$

which is the growing mode of the linear approximation normalized so that  $D(t \rightarrow \infty) = 1$ . Then, the function  $\mathcal{F}(\delta_L, a)$  is given by:

$$\delta_L > \frac{3}{2} D(t) \begin{cases} 1 + \delta = \left( \frac{\cosh \eta_b - 1}{1 - \cos \theta} \right)^3 \left( \frac{\theta - \sin \theta}{\sinh \eta_b - \eta_b} \right)^2 \\ \delta_L = \frac{3}{2} D(t) \left[ 1 + \left( \frac{\theta - \sin \theta}{\sinh \eta_b - \eta_b} \right)^{2/3} \right] \end{cases}$$

and

$$\delta_L < \frac{3}{2} D(t) \begin{cases} 1 + \delta = \left( \frac{\cosh \eta_b - 1}{\cosh \eta - 1} \right)^3 \left( \frac{\sinh \eta - \eta}{\sinh \eta_b - \eta_b} \right)^2 \\ \delta_L = \frac{3}{2} D(t) \left[ 1 - \left( \frac{\sinh \eta - \eta}{\sinh \eta_b - \eta_b} \right)^{2/3} \right] \end{cases}$$

In the case  $\Omega \rightarrow 0$  ( $\eta_b \rightarrow \infty$ ,  $D(t) \rightarrow 1$ ), large overdensities have already collapsed, and we are left with:

$$\Omega = 0 : \quad 1 + \delta = \left( 1 - \frac{2}{3} \delta_L \right)^{-3/2} \quad (24)$$

This simple form for  $\mathcal{F}(\delta_L)$  leads to:

$$P_m(\delta) = \frac{(1 + \delta)^{-5/3}}{\sqrt{2\pi}\Sigma(M)} \exp \left[ -\frac{9}{8\Sigma^2} \left( 1 - (1 + \delta)^{-2/3} \right)^2 \right] \quad (25)$$

which provides a convenient estimation for  $P_m(\delta)$ . As for a critical universe we can still define a generating function  $\varphi_m(y, \bar{\xi}_m)$  which allows us to recover the results of Bernardeau (1994a).

### 2.2.2. Eulerian point of view

Naturally, we can obtain an approximation for the probability distribution  $P(\delta)$  of the density contrast within cells of scale  $R$  in a fashion similar to what we did for a critical universe from the Lagrangian probability  $P_m(\delta)$ . In the case of a power-spectrum which is a power-law, and in the limit  $\Omega \rightarrow 0$ , we get for instance:

$$P(\delta) = \frac{(1 + \delta)^{(n-9)/6}}{4\sqrt{2\pi}\Sigma(R)} \left[ n + 3 + (1 - n)(1 + \delta)^{-2/3} \right] \times \exp \left[ -\frac{9(1 + \delta)^{(n+3)/3}}{8\Sigma^2} \left( 1 - (1 + \delta)^{-2/3} \right)^2 \right] \quad (26)$$

As we shall see in the next section, this very simple formula provides in fact a good approximation to  $P(\delta)$  for all values of  $\Omega$  of interest (even for  $\Omega = 1$ ) due to the weak dependence of  $\mathcal{F}(\delta_L, \Omega)$  on  $\Omega$ . As for a critical universe we can also define a generating function  $\varphi(y, \bar{\xi})$  and recover the results of Bernardeau (1994a).

We can note that Protogeris & Scherrer (1997) obtained similar results with an approach close to ours. They considered ‘‘local Lagrangian approximations’’ where the density contrast at the Lagrangian point  $\mathbf{q}$ , time  $t$ , is related to its initial value by  $\delta = \mathcal{F}(\delta_L)$ . They used several approximations for  $\mathcal{F}$  including the simplified spherical collapse model (24) and obtained the probability distribution (26), which they modified by introducing an ad-hoc multiplicative function  $N(t)$  within the relation  $\delta_L \rightarrow (1 + \delta)$  in order to normalize properly  $P(\delta)$ . However, our model differs from theirs by some aspects. Thus, our Lagrangian probability distribution is defined from the start with respect to a given mass scale  $M$  (which might be seen as a ‘‘smoothing’’ scale). This appears naturally in our approach, and it ensures we always work with well-defined quantities. Indeed, for a power-spectrum which is a pure power-law with  $n > -3$  the ‘‘unsmoothed’’ density field is not a function but a distribution. In fact, one cannot characterize a point by a finite density, without specifying the scale over which this density is realised. Then, the change from the Lagrangian to the Eulerian view-point is quite natural, and it provides an Eulerian distribution function which differs from the Lagrangian one in a very simple and physical manner and which depends on the power-spectrum. No smoothing procedure needs to be applied in fine in order to compare with observations: a filtering scale ( $M$  or  $R$ ) is always automatically included in our approach. Our approximation also shows clearly the dependence on  $\Omega$  of the functions  $\mathcal{F}(\delta_L)$  and  $\varphi(y)$ . Finally, one can note that contrary to Protogeris & Scherrer (1997) we did not normalize our probability distribution  $P(\delta)$ . In fact, we think such a procedure is somewhat artificial and may lead to an even worse approximation. Indeed, if the normalization problem comes mainly from a specific interval of the density contrast where our

approximation is very bad, a simple normalization procedure will not give very accurate results in this interval (since the starting values have no relation with the correct ones) while it will destroy our predictions in the interval where they were fine. Thus, one can fear such “cure” may in fact spread errors over all density contrasts. We shall come back to this point below, but we can already note that for  $n = 1$  the probability distribution (26) cannot be meaningfully normalized since  $\int P(\delta)d\delta = \infty$ .

### 2.3. Comparison with numerical results

From the results of previous paragraphs, since the functions  $\varphi(y)$  obtained with our prescription in the limit  $\bar{\xi} \rightarrow 0$  are exactly those derived by a rigorous calculation we can expect that the probability distribution  $P(\delta)$  we get should provide a good approximation in the linear regime. Thus, Fig.1 and Fig.2 present a comparison of our approximation with the results of numerical simulations, taken from Bernardeau (1994a) and Bernardeau & Kofman (1995) in the case of a CDM initial power-spectrum in a critical universe. We display our predictions for a critical universe (relation (20)) and an “empty” universe (relation (26)), for a power-spectrum which is a power-law with  $n$  given by the local slope of the actual power-spectrum.

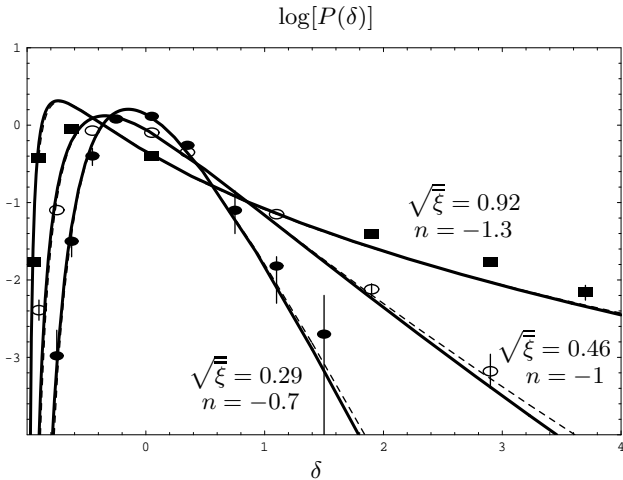


**Fig. 1.** The probability distribution of the density contrast  $P(\delta)$ . The solid lines present the prediction of our prescription for a critical universe and a power-spectrum which is a power-law (relation (16) or (20)), for various  $\bar{\xi}$  and  $n$ , while the dashed-lines show the corresponding curves for an empty universe  $\Omega = 0$  (relation (26)). The data points are taken from Bernardeau (1994a) and Bernardeau & Kofman (1995) and correspond to a numerical simulation with a CDM initial power-spectrum in a critical universe (thus  $n$  is the local slope of the power-spectrum). The density fluctuation  $\bar{\xi}$  and  $n$  were measured in the simulation.

We can see that our approach leads indeed to satisfactory results up to  $\bar{\xi} \sim 1$  given its extreme simplicity.

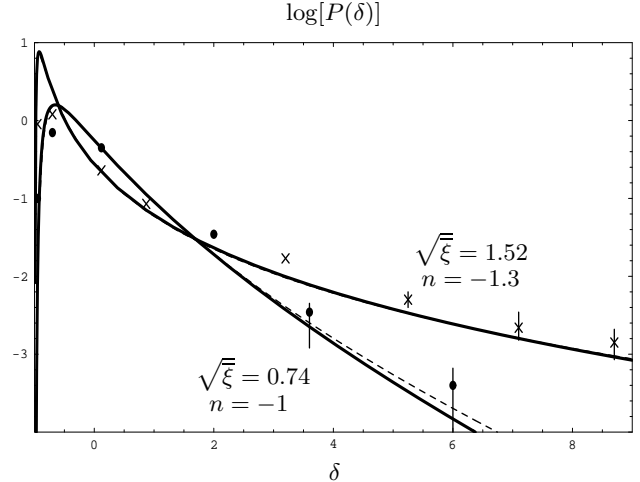


**Fig. 2.** The probability distribution of the density contrast  $P(\delta)$  as in Fig.1 but for two different values of  $\bar{\xi}$ .

As was noticed by Bernardeau (1992), the  $\Omega$  - dependence of the probability distribution is very weak (the dashed lines are very close to the solid lines on the figures), which means that the simple expression (26) provides a reasonable fit for all cosmological models up to  $\bar{\xi} \sim 1$ . However, as we can see on Fig.2, our prescription leads to a sharp peak for very underdense regions  $\delta \simeq -1$  which increases with  $\bar{\xi}$  but does not appear in the numerical results. This defect is also related to the fact that our probability distribution is not correctly normalized to unity. This problem is due to the expansion of underdense regions, which according to the spherical dynamics grow faster than the average expansion of the universe so that in our present model these areas occupy after some time a volume which is larger than the total volume which is available, which leads to a probability which is too large. Indeed, within our approach underdense regions can expand without any limit while in reality this growth is constrained by the fact that on large scales we must recover the average expansion  $\propto a^3$ . Thus, underdensities join together after some time and their mutual influence alters their dynamics, which we did not take into account.

A simple way to normalize correctly the probability distribution  $P(\delta)$  would be to define the latter from the generating function  $\varphi(y, \bar{\xi})$  which one would take identical to  $\varphi(y)$  for any  $\bar{\xi}$ : this is the method used successfully by Bernardeau (1994a). However, there is a priori no fundamental reason why this should be a particularly efficient procedure (except from the mere constatation that it works). In fact, as we can see on Fig.2 we can expect most of the problem to come from the peak which develops at low density contrasts, so that one should keep the consequences of the evolution of  $P(\delta)$ , and  $\varphi(y, \bar{\xi})$ , in other ranges of  $\delta$  and simply disregard the predictions obtained in the vicinity of this peak or introduce a specific modification for this interval. This is even clearer on Fig.3 where we can see that our approximation can still pro-

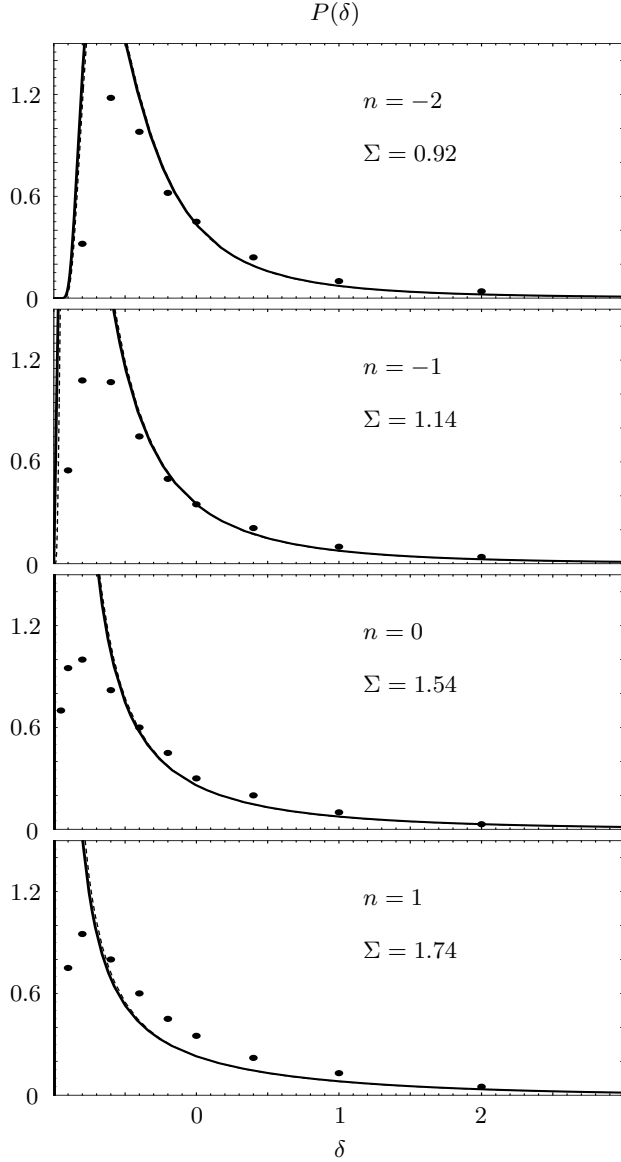


**Fig. 3.** The probability distribution of the density contrast  $P(\delta)$ . The solid lines present the prediction of our prescription for a critical universe and a power-spectrum which is a power-law (relation (16) or (20)), for various  $\Sigma$  and  $n$ , while the dashed-lines show the corresponding curves for an empty universe  $\Omega = 0$  (relation (26)). The data points are taken from Protogeris et al.(1997).

vide reasonable predictions for  $\delta > 0$  and  $\Sigma \simeq 1$  although it completely fails for underdense regions. Of course the agreement with numerical results improves for smaller  $\Sigma$ , as shown on Fig.1 and Fig.2, and becomes excellent in the limit  $\Sigma \rightarrow 0$ . We only show on Fig.3 the largest values of  $\Sigma$  where our approximation still makes some sense, in order to present its range of validity and to show clearly for which values of  $\delta$  (underdensities) it breaks down first. As Protogeris et al.(1997) noticed, the problem becomes increasingly severe as  $n$  gets larger. However, our predictions work better than those used by these authors because we

did not normalize our probability distribution (see their Fig.2). This was expected since we noticed earlier that  $\int P(\delta)d\delta = \infty$  for  $n = 1$ , so that it cannot even be normalized, but this does not prevent our approximation to provide very good results for low  $\Sigma$ , and when  $\Sigma \rightarrow 0$  we recover the gaussian on any finite interval of the density contrast which does not include  $\delta = -1$ .

### 3. Quasi-linear regime: velocity divergence

The prescription we described in the previous paragraphs can also predict the statistical properties of the divergence of the velocity field. Note that we cannot get any reliable result for the shear, since our model is based on a pure spherical dynamics, so that the shear is zero for all the individual regions of matter we consider. This is clearly an important shortcoming of this simple approximation, however in the linear regime where density fluctuations are small the rotational part of the velocity field decays so that after a long time (but still in the linear regime) keeping only the growing mode the velocity can be described by its divergence, or a velocity potential. Thus, our model does not contradict a priori the properties of the linear regime, which is of course a first requisite. We define the peculiar velocity  $\mathbf{v}$  by:

$$\dot{\mathbf{r}} = \mathbf{u} = \dot{a}\mathbf{x} + a\dot{\mathbf{x}} = \frac{\dot{a}}{a}\mathbf{r} + \mathbf{v} \quad (27)$$

and the divergence  $\theta$  ( $\nabla = \partial/\partial\mathbf{x}$  in comoving coordinates, and  $\nabla_r = \partial/\partial\mathbf{r}$ ) by:

$$\theta = \frac{\nabla \cdot \mathbf{v}}{\dot{a}} = \frac{a}{\dot{a}} \nabla_r \cdot \mathbf{v} \quad (28)$$

We can note that in the linear regime, where we keep only the growing mode, we have:

$$\theta = -\delta \frac{a\dot{D}}{\dot{a}D} = -\delta f(\Omega) \quad (29)$$

where  $D(t)$  is the growing mode of the density fluctuations and  $f(\Omega) \simeq \Omega^{0.6}$  (see Peebles 1980).

To use the method we described for the density contrast  $\delta$ , we must now link the divergence  $\theta$  of the velocity field to the linear density contrast  $\delta_L$  of our Lagrangian elements of matter. One possibility is to make the approximation that the density is uniform over these individual regions, and to use the continuity equation (in physical coordinates):

$$\frac{\partial \rho}{\partial t} + \rho \nabla_r \cdot \mathbf{u} = 0 \quad (30)$$

An alternative is to consider the mean divergence over the Lagrangian matter element  $V$ , which can be expressed in terms of the expansion of this global volume (velocity of the outer boundary):

$$\dot{a} \langle \theta \rangle = \frac{1}{V} \int_V (\nabla \cdot \mathbf{v}) d^3x = \frac{1}{V} \int_S \mathbf{v} \cdot \mathbf{ds} \quad (31)$$

This last “definition” of  $\theta$  is the most natural as it does not need any additional information on the density profile. However, in both cases we obtain:

$$\theta = -\frac{d\ln(1+\delta)}{d\ln a} \quad (32)$$

which relates  $\theta$  to  $\delta_L$  through the relation  $\delta = \mathcal{F}(\delta_L, a)$  used in the previous sections (note that the derivative in (32) is to be understood at fixed  $\nu$ : one follows the motion of a given fluid element, so that  $\delta_L$  is also a function of  $a$ ). Then, we obtain the Lagrangian probability distribution  $P_m(\theta) d\theta = -P_L(\delta_L) d\delta_L$  and its Eulerian counterpart, which is simply given by  $P(\theta) d\theta = -P(\delta) d\delta$  (we introduced a negative sign because  $d\theta/d\delta < 0$ ). Thus the latter can be written:

$$P(\theta) = \frac{-1}{\sqrt{2\pi}} \frac{1}{1+\delta} \frac{\partial}{\partial \theta} \left[ \frac{\delta_L}{\Sigma(R_m)} \right] \exp \left[ -\frac{1}{2} \left( \frac{\delta_L}{\Sigma} \right)^2 \right] \quad (33)$$

We can also introduce the functions  $\varphi_{m\theta}(y, \bar{\xi}_{m\theta})$  and  $\varphi_\theta(y, \bar{\xi}_\theta)$  (with  $\bar{\xi}_\theta = \langle \theta^2 \rangle$ ). As was the case for the density contrast we recover in the limit  $\bar{\xi}_\theta \rightarrow 0$  the functions derived by Bernardeau (1994a).

If we make the approximation  $\mathcal{F}(\delta_L, a) = \mathcal{F}_0(\delta_L)$  where  $\mathcal{F}_0$  is the function obtained in the limit  $\Omega \rightarrow 0$  (see (24)) we get:

$$\theta = -f(\Omega) \delta_L \left( 1 - \frac{2}{3} \delta_L \right)^{-1} \quad (34)$$

Then, if we define  $\varpi = \theta/f(\Omega)$  we obtain:

$$P(\theta) d\theta = P(\varpi) d\varpi \quad (35)$$

with

$$P(\varpi) = \frac{1}{\sqrt{2\pi}\Sigma} \left( 1 - \frac{2}{3}\varpi \right)^{(n-11)/4} \left( 1 - \frac{n+3}{6}\varpi \right) \times \exp \left[ -\frac{\varpi^2}{2\Sigma^2} \left( 1 - \frac{2}{3}\varpi \right)^{(n-1)/2} \right] \quad (36)$$

Note that the probability distribution of the reduced variable  $\varpi$  does not depend any longer on the cosmology (we only neglected the slight dependence on  $\Omega$  of the function  $\mathcal{F}$ ).

We compare this approximation (36) to the results of numerical simulations taken from Bernardeau et al.(1997) on Fig.4. We can see that we match the high cutoff of  $P(\theta)$ , which corresponds simply to the expansion rate of a void (zero density), but the negative tail is not well reproduced for the case of the open universe. Thus, it seems that the description of the velocity field is more sensitive on the approximations involved in our method than the density field. This may be due to the influence of the shear, which implies that the velocity can no longer be

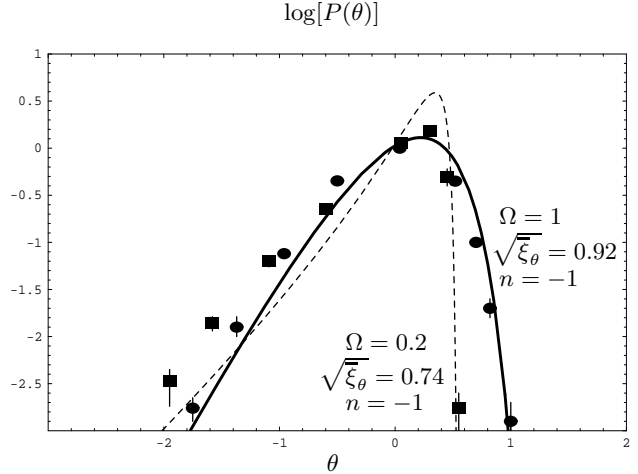


**Fig. 4.** The probability distribution of the divergence of the velocity field  $P(\theta)$ . The solid line is the prediction of our prescription for a critical universe while the dashed-lines corresponds to an open universe  $\Omega = 0.2$ ,  $\Lambda = 0$ . The data points are taken from Bernardeau et al.(1997) for the same conditions (filled circles for the critical universe and rectangles for the open universe).

determined by a mere scalar (through the potential or the divergence). Moreover, we can note that, contrary to the Zeldovich approximation for instance, our prescription does not provide the location of particles and their velocity field from initial conditions (all regions of space cannot follow a spherical dynamics at the same time), it only gives an estimate for some probability distributions without considering the consistent dynamics of all particles simultaneously. Thus, the goal of our approach is more modest than such a global modelization and it is not entirely self-consistent. However, it appears that after accepting this shortcomings we obtain nevertheless reasonable results for the density field. In fact, as we shall see in the next section, we expect large density fluctuations to follow a dynamics close to the spherical model while the intermediate areas which connect these regions obey a complex non-spherical dynamics but as their density contrast is of the order of  $\Sigma$  they do not play an important role for the global shape of  $P(\delta)$  as long as  $\Sigma < 1$ .

#### 4. Spherical density fluctuations

As we showed in the previous paragraphs, the spherical dynamics provides a good approximation to the behaviour of the density field (and a reasonable description for the velocity divergence) in the quasi-linear regime, and it even gives the exact generating functions  $\varphi(y)$  in the limit  $\bar{\xi} \rightarrow 0$ . This may look surprising, since all regions of space cannot follow simultaneously a spherical dynamics as we have already noticed, so that one would expect this prescription to be always somewhat different from the exact results. In fact, as we shall see below, this is due to the fact that the limit  $\bar{\xi} \rightarrow 0$  (or equivalently  $\Sigma \rightarrow 0$ )



constrains the increasingly rare density fluctuations of order unity to be spherically symmetric. Then a spherical dynamics should naturally lead to correct results. Note that the mean evolution before virialization of rare large density fluctuations was treated by Bernardeau 1994b.

Thus, let us define  $\delta_L$  (resp.  $\delta'_L$ ) as the mean density contrast over a sphere of radius  $R$  (resp.  $R'$ ) centered on a point  $O$  (resp.  $O'$ ), and we note  $\mathbf{r}$  the vector  $\overrightarrow{OO'}$ . Then, the conditional probability  $P(\delta'_L|\delta_L) d\delta'_L$  to get a density contrast  $\delta'_L$  knowing that we have a density contrast  $\delta_L$  in the first sphere is simply a gaussian:

$$P(\delta'_L|\delta_L) = \frac{1}{\sqrt{2\pi\Sigma_0}} e^{-(\delta'_L - \delta_{L0})^2 / (2\Sigma_0^2)} \quad (37)$$

where we defined:

$$\Sigma^2 = \int_0^\infty dk 4\pi k^2 W(kR)^2 P(k) \quad , \quad \Sigma' = \Sigma(R')$$

$$\Sigma''^2 = \int_0^\infty dk 4\pi k^2 W(kR)W(kR') P(k) \frac{\sin(kr)}{kr}$$

hence  $\Sigma = \langle \delta_L^2 \rangle$ ,  $\Sigma' = \langle \delta_L'^2 \rangle$ ,  $\Sigma'' = \langle \delta_L \delta_L' \rangle$

$$\text{and } \delta_{L0} = \delta_L \frac{\Sigma''^2}{\Sigma^2} \quad , \quad \Sigma_0^2 = \frac{\Sigma^2 \Sigma'^2 - \Sigma''^4}{\Sigma^2}$$

and  $W(x) = 3(\sin x - x \cos x)/x^3$  is the top-hat window function (see for instance Bardeen et al.1986 for properties of gaussian random fields). Thus, the mean value of  $\delta'_L$  is  $\delta_{L0}$  which only depends on the distance  $r = |\mathbf{r}|$  from the point  $O$  where the density contrast is constrained to be  $\delta_L$  over  $R$ , which is obvious from the symmetry of the problem. However, the profile of the density fluctuation centered on  $O$  is usually not spherically symmetric, because of the fluctuations of  $\delta'_L$ . If we consider now the limit  $\Sigma \rightarrow 0$  (i.e. the normalization of the power-spectrum goes to 0) at fixed  $\delta_L$ , the mean value  $\delta_{L0}$  does not change but  $\Sigma_0 \rightarrow 0$ . Thus, in this limit the profile of the density fluctuation centered on  $O$  becomes spherically symmetric ( $\delta'_L(\mathbf{r}) = \delta_{L0}(|\mathbf{r}|)$ ), and its dynamics is exactly described by the spherical model we used in the previous paragraphs. Of course, most of the matter (and space) is formed by density fluctuations  $|\delta_L| \sim \Sigma$  which are not spherically symmetric, but these areas correspond by definition to density contrasts which tend to 0 as  $\Sigma \rightarrow 0$  and they do not influence the shape of the functions  $\varphi(y)$  which depend on finite values of the density contrast. This can be seen for instance on (10) which shows that a finite value of  $y$  corresponds to a finite value of the density contrast  $\delta_y$  given by  $\delta_y = -y \mathcal{F}'(\delta_y)$  while  $\Sigma \rightarrow 0$ . Thus, our approach explains the results of the rigorous calculation of the generating functions  $\varphi(y)$  in the limit  $\Sigma \rightarrow 0$  from the exact equations of motion, and why they depend simply on the spherical dynamics. Moreover, our model is not restricted a priori to  $\Sigma \ll 1$  and the comparison with numerical simulations shows it gives reasonable results up to  $\Sigma \sim 1$ .

## 5. Non-linear regime

We showed in the previous paragraphs that a very simple model, based on the spherical dynamics, can describe the evolution of the density field up to  $\bar{\xi} \sim 1$ . It is very tempting to try to extend this model into the non-linear regime up to  $\bar{\xi} \sim 200$ , which is sufficient to describe approximately the subsequent highly non-linear regime with the help of the stable-clustering ansatz (e.g. Peebles 1980 for a description of this latter approximation). However, this implies that we take into account other processes like virialization, which can only be made in a very crude way within the framework of the prescription described in the previous paragraphs, so that we cannot hope to get accurate quantitative results. In fact, this highly non-linear regime where the probability distribution of the density contrast is governed by the properties of virialized objects is probably beyond the reach of rigorous perturbative methods based on the expansion of the equations of motion given by a fluid description with an irrotational velocity field. Indeed, the fluid approximation itself breaks down after shell-crossing and cannot describe collapsing halos, so that one has to use the Liouville equation which makes the analysis more difficult. Hence it may still be worthwhile to consider simple models like the one described in this article which could give some hindsight into the relevant processes.

### 5.1. Spherical collapse

#### 5.1.1. Counts-in-cells

According to the spherical dynamics large overdensities decouple slowly from the general expansion of the universe, reach a maximum radius  $R_m$ , turn-around and collapse to a singularity when their linear density contrast  $\delta_L$  is equal to a critical value  $\delta_c$ , with  $\delta_c \simeq 1.69$  for  $\Omega = 1$  (we shall only consider the case of a critical universe in the following). However, one usually assumes that such an overdensity will eventually virialize (because the trajectories of particles are not purely radial) into a finite radius to form a relaxed halo. Generally, this virialization radius  $R_v$  is taken to be one half of the turn-around radius, from arguments based on the virial theorem, so we shall note  $R_v = \alpha/2 R_m$  with  $\alpha \sim 1$ . If we assume that after virialization this halo remains stable, its density contrast will grow as  $a^3$ , while its ‘‘linear’’ density contrast increases as  $a^2$ . Thus, we modify the function  $\delta = \mathcal{F}(\delta_L)$  which links  $\delta_L$  to  $\delta$  so that:

$$\delta_L \geq \delta_c : 1 + \delta = \left(\frac{10}{3\alpha}\right)^3 \delta_L^3 \quad (38)$$

At the time of collapse where the linear density contrast  $\delta_L$  is equal to  $\delta_c$ , the actual density contrast of the halo is  $1 + \delta = \alpha^{-3} (1 + \Delta_c) \simeq \alpha^{-3} 178$ . Within the framework

of stable clustering, a similar relation can be obtained for  $\bar{\xi}$  (see VS):

$$\bar{\xi} > 200 : \bar{\xi}(R) \simeq \left(\frac{10}{3\alpha_\xi}\right)^3 \bar{\xi}_L(R_L)^3 \quad (39)$$

where  $R_L$  is related to  $R$  in a fashion similar to  $R_m$

$$R_L^3 = (1 + \bar{\xi}) R^3 \quad (40)$$

which comes from the fact that these approximations are based on a Lagrangian point of view where one follows the evolution of matter elements of constant mass. One can expect  $\alpha_\xi \neq \alpha$  since all regions of space do not follow the same dynamics, and in fact the previous model only applies to overdensities, which form one half of the volume and mass in the early linear universe. Then, in a fashion similar to what was done in VS, we obtain using (16):

$$P(\delta) = \frac{1}{\bar{\xi}^2} \frac{1}{\sqrt{2\pi}} \frac{5+n}{6} \frac{\alpha}{\alpha_\xi} \left(\frac{\delta}{\bar{\xi}}\right)^{(n-7)/6} \times \exp \left[ -\frac{\alpha^2}{2\alpha_\xi^2} \left(\frac{\delta}{\bar{\xi}}\right)^{(5+n)/3} \right] \quad (41)$$

so that the probability distribution of the density contrast satisfies the scaling-law:

$$P(\delta) = \frac{1}{\bar{\xi}^2} h(x) \quad \text{with} \quad x = \frac{1+\delta}{\bar{\xi}} \quad (42)$$

since in the regime we consider here ( $\delta > 200, \bar{\xi} > 200$ ) we have  $(1+\delta)/\bar{\xi} \simeq \delta/\bar{\xi}$ . The variable  $x$  is related to the usual linear parameter  $\nu$  by:

$$\nu = \frac{\alpha}{\alpha_\xi} x^{(5+n)/6} \quad (43)$$

while the scaling function  $h(x)$  is simply:

$$x^2 h(x) = \frac{1}{\sqrt{2\pi}} \frac{5+n}{6} \frac{\alpha}{\alpha_\xi} x^{(5+n)/6} \exp \left[ -\frac{\alpha^2 x^{(5+n)/3}}{2\alpha_\xi^2} \right] \quad (44)$$

In fact, this scaling is characteristic of a much wider class of models, defined by the scale-invariance of the many-body correlation functions, studied in detail by Balian & Schaeffer (1989). Thus, the model we described in this article, based on the spherical dynamics and a strong stable clustering assumption, appears as a simple way to estimate the scaling function  $h(x)$  characteristic of the highly non-linear regime. Then, all the analysis developed for this general class of density fields can be applied to this peculiar model. As was noticed in VS, the approach presented in this article allows one to recover the PS mass function as it is based on the same fundamental idea: one follows the evolution of individual matter elements from the linear regime, described by gaussian probability distributions,

into the non-linear regime. Indeed, if in a fashion similar to PS we identify the fraction  $F(> M)$  of matter embedded within just-virialized objects of mass larger than  $M$  with the mass contained in cells of scale  $R$  with a density contrast  $\delta > \Delta_{c\alpha}$  (with  $(1 + \Delta_{c\alpha}) = \alpha^{-3} \Delta_c \simeq \alpha^{-3} 178$  and  $M = (1 + \Delta_{c\alpha})\bar{\rho}V$ ) we obtain:

$$F(> M) = F(> \Delta_{c\alpha}, R) = F_L(\delta_c, R_m) \quad (45)$$

Here  $F_L$  is the fraction of matter computed in the linear gaussian field, and we used the fact that in our spherical model a density contrast  $\delta_L$  over a scale  $R_m$  in the initial gaussian random field is associated to a density contrast  $\delta = \mathcal{F}(\delta_L)$  over a scale  $R$  in the actual non-linear density field as described in (13) and (15), as in the PS prescription. Then, the mass fraction in collapsed objects of mass  $M$  to  $M + dM$  is simply:

$$\begin{aligned} \mu(M) \frac{dM}{M} &= -\frac{\partial}{\partial R} F(> \Delta_{c\alpha}, R) dR \\ &= -\frac{\partial}{\partial R_m} F_L(> \delta_c, R_m) dR_m \end{aligned} \quad (46)$$

Since we have  $F_L(> \delta_c, R_m) = P_L(> \delta_c, R_m)$  we recover as we should the PS mass function:

$$\mu(M) \frac{dM}{M} = \frac{1}{\sqrt{2\pi}} \frac{\delta_c}{\Sigma} \left| \frac{d \ln \Sigma}{d \ln M} \right| e^{-\delta_c^2/(2\Sigma^2)} \frac{dM}{M} \quad (47)$$

However, (41) is not strictly equivalent to the usual PS prescription, since in addition to the spherical model it also relies on stable clustering. One should note that we did not multiply our probability distribution by the usual factor 2, so that we only recover one half of the total matter content of the universe since the previous arguments only apply to initial overdensities. Hence the scaling function (44) verifies  $\int x h(x) dx = 1/2$  while this integral should be normalized to unity. This implies (at least) that the approximate  $h(x)$  we obtained cannot be used for any  $x$ . In fact, following the discussion of Sect.4, we expect the spherical dynamics model we used so far to be valid only for extreme events  $|\nu| \gg 1$ . Hence the approximate  $P(\delta)$  and  $h(x)$  we got should only apply to  $x \gg 1$ . The normalization problem of the PS mass function is often ‘‘cured’’ by an overall multiplication by a mere factor 2, ‘‘justified’’ by the excursion set approach in the case of a top-hat in  $k$  (Cole 1989; Bond et al.1991). However, this result does not extend to other window functions (like the top-hat in real space used here) with which for large overdensities  $\nu \gg 1$  the PS mass function does not suffer from the cloud-in-cloud problem in the sense that the multiplicative factor needed to correct for double counting goes to 1 (and not 2) for large masses (Bond et al.1991; Peacock & Heavens 1990; VS). Hence, it appears that one should not multiply (44) by 2, but merely restrict its application to  $x \gg 1$ . Moreover, we can note that this normalization problem is closely related to the behaviour of underdensities, which are not well described in the usual PS approach

and constitute the missing half of the matter content of the universe.

### 5.1.2. Density profile of virialized halos

We can notice that an overdensity with an initial density profile which is exactly given by the mean value  $\delta_{L0}$  (Sect.4) leads to a final virialized halo with a flat slope in its inner parts, since the initial density contrast  $\delta'_L$  converges to a finite value at the center ( $R' \rightarrow 0$  in the case  $r = 0$ ). This is not consistent with the results obtained from numerical simulations which find inner density profiles  $\rho \propto r^{-1}$  (Navarro et al.1996; Navarro et al.1997; Torren et al.1997) or even steeper (Moore et al.1998). However, for moderate values of  $\nu$  the correlation between the density at scale  $R$  and the density at a smaller scale  $R'$  enclosed within the former one quickly weakens as the fluctuation  $\Sigma_0 \sim \Sigma'$  becomes larger than  $\delta_{L0}$  ( $\Sigma'$  diverges for small  $R'$  while  $\delta_{L0}$  remains finite). As a consequence one cannot infer the average density profile of virialized halos from  $\delta_{L0}$ . In fact, it seems more reasonable to consider an initial density profile of the form:

$$\delta_L \propto \Sigma \propto x^{-(n+3)/2} \quad (48)$$

which leads to a final density profile for the virialized halo:

$$(1 + \delta) \propto \rho \propto R^{-\gamma} \quad \text{with} \quad \gamma = \frac{3(3+n)}{5+n} \quad (49)$$

where  $x$  (resp.  $R$ ) is a comoving (resp. physical) coordinate. The reasoning below (48) is that if we look at a virialized halo of mass  $M$ , its characteristic density within a smaller sphere of mass  $M'$  (centered on the peak) will be set by the maximum linear density contrast  $\delta'_L$  realised over all spheres of mass  $M'$  enclosed within the larger matter element  $M$ . The value of this maximum  $\delta'_{Lmax}$  will scale with  $M'$  as  $\Sigma'$ , as soon as  $\Sigma' \gg \Sigma$ , see (37), which leads to (48). This picture also assumes that during virialization new collapsing shells which may not be centered on the density peak will roughly circularize around it. We can note that for  $-2 < n < -1$  the slope (49) is  $1 < \gamma < 1.5$  which is close to what is seen in simulations (Navarro et al.1997; Moore et al.1998a). The same reasoning could also be applied to underdensities, which we shall use in the next section. However, the previous arguments are quite crude and a much more detailed analysis would be required to get a good description of virialized halos. Moreover, within the approach described in the previous section the shape of the mean density profile has a rather weak meaning since the model implies that a lot of substructure is present within halos, so that a large object can be decomposed as a hierarchy of many smaller peaks with larger densities. Note that some simulations (Ghigna et al.1998) seem indeed to show that many sub-halos can survive within larger objects although not to such a large extent as in the model (this might be due to finite resolution effects).

## 5.2. Underdensities

### 5.2.1. Density profile of underdensities

The function  $x^2 h(x)$  obtained in the previous section (44) seems to show that the exponent of the small  $x$  power-law tail is  $\omega = (5+n)/6$ . However, as we argued above we do not expect this scaling function to give reasonable results for  $x \ll 1$ , so that we need to get  $\omega$  from another point of view, which considers explicitly low-density regions. Indeed, since we expect the spherical dynamics approximation to be valid mainly for rare events we shall shift from  $\nu \gg 1$  to  $\nu \ll -1$ : that is we now study very underdense areas. Moreover, initially non-spherical underdensities tend to become increasingly spherical as they expand (contrary to the collapse which enhances deviations from spherical symmetry), as seen in Bertschinger (1985), so that a spherical dynamics model could give reasonable results. We shall assume in this paragraph that the many-body correlation functions are scale-invariant, so that the density field is described by the scaling function  $h(x)$  in the non-linear regime  $\bar{\xi} \gg 1$  for  $(1+\delta) \gg \bar{\xi}^{-\omega/(1-\omega)}$  which includes very underdense and small  $x$  regions. Then, if we consider a sphere of radius  $R$  with a density contrast  $\delta$  over  $R$ , the mean density contrast  $\langle 1 + \delta' \rangle_\delta >_\delta$  on its outer shell can be shown to be:

$$x \ll 1 : \langle 1 + \delta' \rangle_\delta = \left( 1 + \frac{\gamma}{3} \frac{\omega}{1-\omega} \right) (1 + \delta) \quad (50)$$

for low density regions ( $(1 + \delta) \ll \bar{\xi}$ ), where

$$\gamma = \frac{3(3+n)}{5+n} \quad (51)$$

is the slope of the two points correlation function in the highly non-linear regime and  $n$  is the slope of the initial power-spectrum  $P(k)$  which we assume here to be a power-law. This means that the density profile is locally  $\rho \propto R^{\gamma\omega/(1-\omega)}$ . Thus, to get  $\omega$  we may consider the evolution of the density profile of a typical spherical underdensity using (50). Let us follow an underdensity with an initial profile in the early universe  $|\delta_L| \propto \Sigma(M) \propto M^{-(n+3)/6}$  (see (48)). Its dynamics is simply given by the spherical model:

$$\begin{cases} R = A(\cosh \eta - 1) \\ t = B(\sinh \eta - \eta) \end{cases} \quad \text{with} \quad A^3 = \mathcal{G}MB^2 \quad (52)$$

and

$$\delta_L(t) = -\frac{3}{20} \left( \frac{6t}{B} \right)^{2/3} \quad (53)$$

Hence we have:

$$\begin{cases} B \propto |\delta_L|^{-3/2} \\ A \propto M^{1/3} B^{2/3} \propto |\delta_L|^{-(n+5)/(n+3)} \end{cases} \quad (54)$$

At late times  $\eta \gg 1$ , and using (3) we obtain:

$$\begin{cases} R \sim A \cosh \eta \sim A t/B \sim |\delta_L|^{(n-1)/(2(3+n))} \\ (1 + \delta) \sim 1/\cosh \eta \sim B \sim |\delta_L|^{-3/2} \end{cases} \quad (55)$$

which means that  $(1 + \delta) \propto R^{3(3+n)/(1-n)}$ . If we identify this exponent with  $\gamma\omega/(1 - \omega)$  we obtain eventually:

$$\omega = \frac{5 + n}{6} \quad (56)$$

which is also the value one would have inferred from (44). We can note that although the initial density is lower in the central regions of the perturbation, which expand faster, there is no shell-crossing and the density profile is given by (55) for  $n < 1$  (the profile of the initial density contrast is less steep than  $\delta_L \propto R^{-2}$ ). As we could expect from the analysis we developed in the linear regime, we can note that the case  $n = 1$  leads to some problems since we would have  $\omega = 1$ . Hence it cannot be described by this simple model. We shall only consider  $-3 < n < 1$ , which corresponds to hierarchical clustering and cosmologically relevant power-spectra (but one may expect that  $n \rightarrow 1$  on very large scales  $R \rightarrow \infty$ ).

### 5.2.2. Contact of underdensities

We shall now develop a slightly more detailed description of the fate of underdensities, in order to follow the behaviour of the matter (one half of the total mass) which was initially embedded in these low-density areas. This means that we have to modify the function  $\mathcal{F}(\delta_L)$  for  $\delta_L < 0$  too. As we noticed in Sect.2, underdensities grow very fast according to the spherical dynamics which leads to an approximate probability distribution of the density contrast with an ever increasing normalization (instead of unity). In fact, the volume formed by any given range of underdensities will eventually outgrow the available volume of the universe within the approximation used so far. Indeed, we can write (14) and (16) as:

$$P(\delta) d\delta = \frac{1}{\sqrt{2\pi}} \frac{1}{1 + \delta} e^{-\nu^2/2} d\nu \quad (57)$$

with

$$\nu = \frac{\delta_L}{\Sigma(R_m)} = \frac{(1 + \delta)^{(3+n)/6} \delta_L}{\Sigma(R)} \quad (58)$$

The linear variable  $\nu$  defines the underdensities as it is a constant of the dynamics. We can see from (57) that a logarithmic interval of  $|\nu|$  of order unity will occupy all the volume of the universe when

$$\frac{1}{\sqrt{2\pi}} \frac{|\nu|}{1 + \delta} e^{-\nu^2/2} \sim 1 \quad (59)$$

Naturally, we cannot keep our model unchanged for later times, since the mean volume of these underdensities

should not grow faster than  $a^3$  after this date. In fact, in this picture such a range of negative density fluctuations first expands following the spherical dynamics until neighbouring underdensities come into contact and fill the entire universe. At this time the universe appears to be constituted of low density bubbles of size  $R$  and density  $\rho$  (with  $\rho < \bar{\rho}$ ). The matter which was “pushed” by these “voids” to form the interface between adjacent underdensities gets squeezed and reaches high densities. Thus, we shall assume the latter build virialized structures of size  $\sim R$  and density  $\sim \rho$  (for instance they may have a density  $\sim 200$  times higher than the density  $\rho$  of neighbouring areas). These represent the sheets and filaments one can observe in numerical simulations (e.g. Bond et al.1996) which separate low-density regions, while the spherical overdensities described in the previous sections are the nodes which form at their intersections (note that the latter, corresponding to large positive initial density fluctuations, appear first). To see more clearly what this would imply for the probability distribution of the density contrast (and for the mass functions) we shall simply consider that underdensities defined by their linear parameter  $\nu$ , and their scale  $R$ , stop expanding when:

$$\frac{|\nu|}{1 + \delta} e^{-\nu^2/2} = \beta \quad (60)$$

with  $\beta \sim 1$  (that is when they fill all of the universe) and keep after this date a constant radius  $R$  and density  $\rho$ . Thus, as time goes on the universe gets filled with increasingly large and underdense “bubbles” while a growing fraction of the matter progressively forms virialized structures (with a characteristic density which becomes vanishingly small as compared to the mean density). Note that within such a picture all the mass will eventually be embedded in virialized high density objects, so that the usual normalization problem is solved in a natural way. Thus, we must now use (60) to obtain a relation  $\nu - \delta$  in order to get the probability distribution of the density contrast from (57). A negative density fluctuation  $\nu$  “stops” when it reaches a density contrast  $\delta_s$  on a scale  $R$  such that  $\Sigma = \Sigma_s$ , defined by (58) and (60). At late times,  $\eta \gg 1$ , the spherical dynamics (see (3)) leads to the approximate relation:

$$(1 + \delta) = \left( \frac{20}{27} |\nu| \Sigma(R) \right)^{6/(n-1)} \quad (61)$$

hence we obtain:

$$\begin{cases} (1 + \delta_s) = \frac{|\nu|}{\beta} e^{-\nu^2/2} \\ \Sigma_s = \frac{27}{20} \beta^{(1-n)/6} |\nu|^{(n-7)/6} e^{(1-n)\nu^2/12} \end{cases} \quad (62)$$

Note that the scale  $R$  is not the Lagrangian scale  $R_m$ , and  $\nu\Sigma(R) \neq \delta_L$ . After this “stopping time”  $t_s$ , the radius of the object does not evolve any longer while its density

contrast increases as  $a^3$ , hence initial underdensities which have already “stopped” verify:

$$(1 + \delta) = (1 + \delta_s)(\nu) \left( \frac{\Sigma(R)}{\Sigma_s(\nu)} \right)^{6/(5+n)} \quad (63)$$

since  $\Sigma(R) \propto a^{(5+n)/2} R^{-(n+3)/2}$  by definition, where  $R$  is the physical radius. This is the relation  $\nu - \delta$  we needed to derive the probability distribution of the density contrast. We can note that the density contrast is now a function of both  $\delta_L$  and  $\Sigma$ , contrary to the pure spherical dynamics case used previously where we had  $\delta = \mathcal{F}(\delta_L)$ . This is in fact a necessary condition to be able to get eventually all the mass of the universe within overdense virialized structures. Finally, this leads to:

$$P(\delta) \simeq \frac{1}{\bar{\xi}^2} \frac{\omega}{\sqrt{2\pi}} \frac{9\beta}{2\alpha\xi} \left[ -2 \ln \left( \frac{9\beta}{2\alpha\xi} x^\omega \right) \right]^{-3/2} x^{\omega-2} \quad (64)$$

where  $\omega$  is defined by (56),  $x$  by (42) and we used (39) to introduce  $\bar{\xi}$ . Thus, we recover the scaling-law (42) with the same exponent  $\omega$  as previously, with logarithmic corrections. Such logarithmic terms may indeed exist, but our model is probably too crude to give a reliable estimate of their importance. As was the case for overdensities, we also obtain a relation between the linear and non-linear parameters  $\nu$  and  $x$ :

$$\nu^2 e^{-\nu^2/2} = \frac{9\beta}{2\alpha\xi} x^\omega \quad (65)$$

This scaling (42) of  $P(\delta)$  applies to density contrasts larger than the one of underdense regions which are currently on the verge of filling the entire universe:  $(1 + \delta) > (1 + \delta_s)$  with:

$$(1 + \delta) > (1 + \delta_s) \sim (\ln \bar{\xi})^{1/(2\omega-2)} \bar{\xi}^{-\omega/(1-\omega)} \quad (66)$$

hence

$$x \gg \bar{\xi}^{-1/(1-\omega)} \quad (67)$$

which is exactly the limit predicted by a general study of the models defined by the scale-invariance of the many-body correlation functions. Thus, the approach developed in this section “explains” in a natural way both the emergence of the scaling-law (42) for small  $x$  and its range of validity. Note that (44) derived from the behaviour of overdensities only applied to virialized objects  $\delta > 200$ , and was in fact restricted to  $x \gg 1$  as we argued above. The previous considerations also mean that, when seen on comoving scale  $x$  at a time defined by the scale factor  $a$ , the universe appears to be covered by very underdense regions of typical density contrast  $\delta_s$  with (omitting logarithmic terms):

$$(1 + \delta_s) \sim \Sigma(x, a)^{6/(n-1)} \sim a^{6/(n-1)} x^{3(n+3)/(1-n)} \quad (68)$$

as long as one remains in the non-linear regime ( $\Sigma(x, a) \gg 1$  that is  $(1 + \delta_s) \ll 1$ ). The “overdensity”  $(1 + \delta_s)$  tends to 0 for large times or small scales as it should, while the volume occupied by most of the matter becomes increasingly negligible.

### 5.2.3. Adhesion model

We shall now try to compare the approach developed above to a very different point of view: the adhesion model, in the peculiar case of 1-dimensional fluctuations (in a 3-dimensional universe). Indeed, from the picture developed in the previous paragraphs we do not expect the adhesion model to give reliable estimates for the counts-in-cells at large values of  $x > 1$ , since in this range we should count roughly spherical virialized halos which have a radius larger than the considered scale  $R$ : these correspond to the overdensities described by the spherical collapse seen in Sect.5.1. Hence the finite value of the virialization radius of these objects plays a crucial role in the final probability distribution of the density contrast, which is then out of reach of the adhesion model where this radius is simply zero. However, this model could give a fairly good picture of the filaments and sheets which characterize the highly non-linear universe as the transverse thickness of these structures, smaller than their length or the radius of the neighbouring “bubbles”, does not play an important role on the counts-in-cells realised at these latter scales. More precisely, we shall try to evaluate the typical density contrast seen on a given scale: this corresponds to the maximum of  $P(\delta)$  and to the density contrast  $\delta_s$  of the “bubbles” which cover the universe.

We shall first consider 1-dimensional density fluctuations, since in this case the Zeldovich approximation is correct until shell-crossing occurs so that we expect the adhesion model to provide reliable results. We still define  $n$  as the index of the power spectrum  $\langle |\delta_k|^2 \rangle \propto k^n$  so that we obtain:

$$-1 < n < 3 : \quad \Sigma(x) \propto a x^{-(n+1)/2} \quad (69)$$

This range in  $n$  ensures that the density fluctuations increase at small scales while the fluctuations of the density potential grow at large scales, so that we are in the domain of the usual hierarchical clustering. We note  $x$  (resp.  $q$ ) the comoving Eulerian (resp. initial Lagrangian) coordinate of particles, in this 1-dimensional problem (at early times  $x \rightarrow q$ ). The relation  $q - x$  is given by the adhesion model for the displacement field, and the density is simply obtained from:

$$\eta(x, a) = \left| \frac{\partial q}{\partial x} \right| = \frac{\partial q}{\partial x} \quad \text{with} \quad \eta = (1 + \delta) \quad (70)$$

We shall follow some of the notations used by Vergassola et al.(1994) and we introduce the reduced velocity  $v$  and velocity potential  $\psi$ :

$$v(x, a) \equiv -\frac{\partial \psi}{\partial x} = \frac{V}{a\dot{a}} \quad (71)$$

where  $V = a\dot{x}$  is the peculiar velocity. We shall only consider the cases  $-1 < n < 1$  where the initial velocity ( $a \rightarrow 0$ ) has homogeneous increments and verifies the scale-invariance:

$$\lambda > 0 : v_0(x+\lambda l) - v_0(x) \stackrel{\text{law}}{=} \lambda^{(1-n)/2} [v_0(x+l) - v_0(x)] \quad (72)$$

while the initial velocity potential satisfies:

$$\lambda > 0 : \psi_0(\lambda x) \stackrel{\text{law}}{=} \lambda^{(3-n)/2} \psi_0(x) \quad (73)$$

with  $v_0(0) = \psi_0(0) = 0$ . Here,  $\stackrel{\text{law}}{=}$  means ‘‘having the same statistical properties’’. Then, the overall density over the cell  $[x_1, x_2]$  is simply:

$$\eta([x_1, x_2], a) = \frac{1}{x_2 - x_1} [q(x_2, a) - q(x_1, a)] \quad (74)$$

where the point  $q(x, a)$  satisfies:

$$\left[ -\frac{q^2}{2} + a\psi_0(q) + xq \right] \text{ is maximum at } q(x, a) \quad (75)$$

as given by the Hopf-Cole solution of the Burgers equation (Hopf(1950), Cole(1951)) obtained from the adhesion model. If there is a shock at the Eulerian location  $x$ , several Lagrangian coordinates  $q$  correspond to the same  $x$  and we choose the smallest one which we note  $q_m(x, a)$ . Then, we have:

$$x = q_m + a v_0(q_m) \quad (76)$$

(which is simply the Zeldovich dynamics). Using (73) we can check that the density  $\eta(\Delta x, a)$  over a cell of size  $\Delta x$  satisfies:

$$\eta(\Delta x, a) \stackrel{\text{law}}{=} \eta(a^{-2/(n+1)} \Delta x, 1) \quad (77)$$

so that one only needs to consider the time  $a = 1$ . The highly non-linear regime which is of interest to us here corresponds to  $a \rightarrow \infty$  or  $\Delta x \rightarrow 0$ . Numerical simulations and theoretical arguments (She et al.1992; Vergassola et al.1994) strongly suggest that the Lagrangian map  $q \rightarrow x(q, 1)$  forms a Devil’s staircase and that shock locations are dense in Eulerian space (for  $-1 < n < 1$ ), which can be proved rigorously for  $n = 0$  (Sinai 1992). Hence for almost every Eulerian coordinate  $x$  a Lagrangian coordinate  $q_m$  exists. Using (76) we can see that for two points  $x_1$  and  $x_2$  at time  $a = 1$  we have:

$$x_2 - x_1 = q_{m2} - q_{m1} + [v_0(q_{m2}) - v_0(q_{m1})] \quad (78)$$

In the limits  $|x_2 - x_1| \rightarrow 0$  and  $|q_{m2} - q_{m1}| \rightarrow 0$  we have from (72) the behaviour  $|v_0(q_{m2}) - v_0(q_{m1})| \sim |q_{m2} - q_{m1}|^{(1-n)/2}$ . Since  $n > -1$  the second term in (78) becomes negligible, so that we expect:

$$\Delta x \sim (\Delta q)^{(1-n)/2} \quad \text{and} \quad \eta^*(\Delta x, 1) \sim (\Delta x)^{2/(1-n)-1} \quad (79)$$

where  $\eta^*$  is the most probable value of  $\eta$  (note however that by definition the mean value of  $\eta$  is simply  $\langle \eta \rangle = 1$ ). Using (77) we obtain:

$$(1 + \delta)^*(\Delta x, a) \sim a^{-2/(1-n)} (\Delta x)^{(1+n)/(1-n)} \quad (80)$$

We shall now consider the approach based on the spherical dynamics we described in the previous sections, applied to this 1-dimensional problem in order to compare its prediction to (80). The equation of motion of a 1-dimensional density fluctuation, of longitudinal size  $2R$ , centered on the origin, in an universe invariant by transverse translations, can be written:

$$\ddot{R} = \frac{4}{9} \frac{R}{t^2} - \frac{2}{3} \frac{R_b}{t^2} \quad (81)$$

where  $R_b$  corresponds to the Hubble expansion of the matter element:  $R_b \propto a$  and  $R/R_b \rightarrow 1$  as  $t \rightarrow 0$  (on the other hand the comoving transverse coordinates remain constant in time). Thus,  $x = R/R_b$  is the comoving coordinate of the outer front which we normalized so that  $x \rightarrow 1$  for  $t \rightarrow 0$ . We can write (81) as:

$$3 t^2 \ddot{x} + 4 t \dot{x} - 2 x + 2 = 0 \quad (82)$$

The solution of this equation is simply related to the initial conditions by:

$$x = 1 + \left( \frac{t}{t_*} \right)^{2/3} \quad \text{and} \quad \delta_L = - \left( \frac{t}{t_*} \right)^{2/3} \quad (83)$$

where  $\delta_L$  is the linear theory density contrast. Indeed, we have  $(1 + \delta) = R_b/R = 1/x$ . Thus, we obtain:  $(1 + \delta) = (1 - \delta_L)^{-1}$ , so that at late times:

$$(1 + \delta) \ll 1 : (1 + \delta) \simeq |\delta_L|^{-1} \quad (84)$$

The linear parameter  $\nu$  is still given by  $\nu = \delta_L/\Sigma(R_m)$  where now  $R_m = (1 + \delta)R$  so that:

$$(1 + \delta_s) \sim (|\nu|\Sigma(R))^{2/(n-1)} \quad (85)$$

Hence according to the model described in the previous section underdensities stop expanding and fill the entire universe when they reach the density contrast  $\delta_s$  such that:

$$(1 + \delta_s) \sim a^{-2/(1-n)} x^{(1+n)/(1-n)} \quad (86)$$

where we omitted logarithmic corrections and we used (69). Here,  $x$  is the considered comoving scale we noted  $\Delta x$  in (80). Thus we recover exactly the behaviour seen above within the framework of the adhesion model (80). This is due to two effects: i) in such a 1-dimensional problem the Zeldovich approximation gives the *exact* dynamics until a shock appears, ii) the formation of these large underdensities corresponds to peaks of the initial velocity potential which are global maxima over a large scale but all particles located in the final broad low-density areas come

from a small Lagrangian region (the peak of  $\psi_0$ ) so that inner properties are given by *local* characteristics and the spherical model is reasonable (the stop of the expansion at  $\delta_s$  models the global constraints, related to the fact that these peaks are only maxima over a finite scale). In fact, both models lead to very similar pictures: most of the universe is filled by the expansion of initial low-density peaks while most of the mass is squeezed between this underdensities in virialized objects (for the spherical model) or infinitesimally thin shocks (in the adhesion model).

For the usual 3-dimensional case, the adhesion model does not lead to the same results as the spherical prescription and there would be a break at  $n = -1$  (while it occurs at  $n = 1$  for both models in the 1-dimensional case): indeed the previous arguments would give  $\omega = (5 + n)/4$  instead of (56) which leads to lower characteristic densities  $(1 + \delta_s)$ . We think this discrepancy could be due to the fact that the Zeldovich approximation does not give the exact dynamics any more, even before a shock forms, so that the shape and size of structures built at late times is not correctly described. Indeed, within this approximation the physical coordinate  $\mathbf{r}$  of a given particle evolves as:

$$\mathbf{r} = a(\mathbf{q} + a\mathbf{p}) \quad (87)$$

which means that for a spherical underdensity we obtain at late times  $(1 + \delta) \sim t^{-2}$  while the spherical dynamics leads to  $(1 + \delta) \sim t^{-1}$ , see (55). Hence the Zeldovich approximation overestimates the expansion of voids which explains the low  $(1 + \delta_s)$  and the high  $\omega$  it gives. Thus, the adhesion model appears to confirm our spherical prescription for 1-dimensional fluctuations, where the former has a rather firm foundation, which builds confidence in our model which predicts moreover scaling-laws which are actually seen in numerical simulations. For the generic 3-dimensional case, this latter result suggests that our prescription is still valid, while the adhesion model should worsen.

#### 5.2.4. Non-spherical corrections

As we noticed above, we expect the spherical dynamics to describe extreme events  $|\nu| \gg 1$ . Moreover, in the same way as the ‘‘cloud-in-cloud’’ problem is not very important for large overdensities  $\nu \gg 1$ , as noticed in VS, which is necessary for the approach developed in paragraph 5.1, the corresponding ‘‘void-in-void’’ problem disappears for  $\nu \ll -1$  (since the gaussian density field is symmetric under  $\nu \leftrightarrow -\nu$ ) which allows one to use the prescription presented in 5.2.2. However, we can see from (65) that large negative values of  $\nu$  correspond to very small  $x$ . Indeed, with  $\omega \simeq 0.5$  we can check that  $\nu < -4$  leads to  $x < 10^{-6}$ ,  $(1 + \delta_s) < 10^{-3}$  and  $\bar{\xi} > 10^3$ . Thus, the range of  $x$  which can be studied in current numerical simulations

$0.05 < x < 50$  may be too small to recover the power-law tail with exponent  $\omega$  and the exponential cutoff predicted by our approach. Hence, non-spherical corrections may change the value of  $\omega$  obtained in numerical simulations. To get an idea of the magnitude and direction of such effects, we can study the case where underdensities only expand along 1 or 2 directions (planar or cylindrical symmetry) while the other axis remain(s) constant in co-moving coordinates. Thus the 1-dimensional problem considered in the previous section corresponds to the expansion along only one direction, while the spherical model represents a growth along all three axis.

For the 1-dimensional growth, (84) implies that we have  $(1 + \delta_s) \sim \Sigma(M)^{-1}$  where we do not consider logarithmic corrections (i.e.  $|\nu| \sim 1$ ). Using  $R_m = R_b$  and  $\Sigma(R_b) \propto \bar{\xi}(R_b)^{(5+n)/6}$  we obtain  $(1 + \delta_s) \sim \bar{\xi}^{-(5+n)/6}$  on scale  $R_b$  (the smallest scale of the underdense regions). If we write this exponent as  $-\omega/(1 - \omega)$  we get:

$$\text{1-D : } \omega = \frac{5 + n}{11 + n} \quad (88)$$

In a similar fashion, a two-dimensional expansion leads to  $(1 + \delta) \propto |\delta_L|^{-(\sqrt{13}-1)/2}$  and:

$$\text{2-D : } \omega = \frac{(5 + n)(\sqrt{13} - 1)}{(5 + n)(\sqrt{13} - 1) + 12} \quad (89)$$

We compare on Table 3 the values obtained in numerical simulations to these estimations. Thus, although we recover the increase of  $\omega$  with  $n$ , non-spherical corrections appear to be non-negligible. Hence we expect the value of  $\omega$  measured in numerical simulations, which is presently close to the 2-D result, to increase somewhat for smaller  $x$  at smaller scales where  $\bar{\xi}$  is larger, and to get closer to the value (56) obtained from the spherical dynamics model.

**Table 1.** Exponent  $\omega$  for various indexes  $n$  of the power-spectrum. The lines 1D, 2D and 3D corresponds to (88), (89) and (56). The last two lines present the results of numerical simulations: Colombi et al.(1997) for A and Munshi et al.(1998) for B.

$n$	-2	-1	0	1
1D	0.33	0.4	0.45	0.5
2D	0.39	0.46	0.52	0.62
3D	0.5	0.66	0.83	1
A	0.3	0.5	0.65	0.65
B	0.33	0.4	0.55	0.7

### 5.3. General picture

Thus, in the non-linear regime virialized objects should form through two different processes according to our model. First, large overdensities with a roughly spherical shape collapse as in the PS approach to build high-density virialized halos. This corresponds to matter elements described by  $\nu \gg 1$  and  $x \gg 1$ . Second, large underdensities expand until they fill the entire universe and see their dynamics influenced by their interaction with neighbouring “voids”. The matter “pushed” by these regions forms high-density filaments and sheets at their interface, which builds virialized structures of increasingly large scale and low density (increasingly lower than the mean density of the universe). Obviously the dynamics of the filaments and walls cannot be described by a spherical model, but our approach takes advantage of the fact that the low-density “bubbles” they surround may still be described by a spherical dynamics, with the addition of other processes to take into account the global constraints which stop their expansion. This models matter elements with  $\nu \ll -1$  and  $x \ll 1$ . The behaviour of the intermediate fluid elements  $|\nu| \sim 1$  is certainly quite complex and depends on non-local properties through the influence of neighbouring peaks and voids. It is not described by our model and corresponds to the transition interval of the scaling function  $h(x)$  around  $x \sim 1$  from its exponential cutoff to its power-law tail. Note that in the regime  $\Sigma \gg 1$ , low density contrast regions  $|\delta| \ll 1$  are not described by linear theory, even though  $|\delta|$  is small, because of shell-crossing. Thus, our model does not provide as accurate predictions as the PS mass function, but it can be tested in numerical simulations by studying the density profiles of large halos or voids, as well as the asymptotic behaviour of  $h(x)$ . It would also be of interest to follow the evolution of initial extreme matter elements  $|\nu| \gg 1$ . Moreover, we think the explicit description of underdensities is a necessary step, which was not considered in detail in the PS formulation. It ensures in a natural way that all the mass will eventually be embedded within high-density virialized structures (which occupy a negligible volume), so that there is no normalization problem, and it allows to describe the complex structure formed by low-density bubbles, filaments and walls, which is seen in numerical simulations (Cole et al.1997; Weinberg et al.1996; Bond et al.1996). One can note that according to our model, substructures should exist within large overdensities, which is not always seen in numerical simulations. However, as Klypin et al.(1998) argue this may be due to a lack of numerical resolution, moreover substructures do appear through counts-in-cells numerical studies.

In the non-linear regime, we have only considered the case of a critical universe so far. However, in a low-density universe when  $\Omega$  becomes small virialized structures no longer form as the linear growth factor  $D(t)$  tends to a

constant: the density perturbations freeze in comoving coordinate. Thus, on small scales where the density fluctuations are large, structures formed early when  $\Omega \simeq 1$  so that the analysis developed above for a critical universe can be applied. To get the characteristics of virialized structures today at these scales one simply needs to consider these early times and then extrapolate until today using the approximation (which was used throughout above) that virialized structures keep a constant scale and density while the mean density of the universe decreases as  $\bar{\rho} \propto a^{-3}$ . On larger scales, fluctuations will never reach the non-linear regime since  $\Sigma$  tends to a constant as  $t \rightarrow \infty$ , which is nearly reached as soon as  $\Omega \sim 0.1$ . Hence, on these scales one can simply use the quasi-linear description developed in Sect.2.2. Thus, one gets a complete picture of the density field in a low-density universe (except for a transitory range where  $\bar{\xi} \sim 10$ ) within the framework of the approximation developed in this article.

## 6. Conclusion

Thus, in this article we have developed a simple model for hierarchical clustering based on a spherical dynamics. We have shown it provides a reasonable approximation to the density field, and the divergence of the velocity field, in the quasi-linear regime  $\Sigma < 1$ . Moreover, it allows one to recover the exact series of the moments of the probability distribution of the density contrast in the limit  $\bar{\xi} \rightarrow 0$  (contrary to other models like the Zeldovich approximation for instance), and sheds some light on the rigorous results. Then, we have developed a way to extend this model into the non-linear regime, by taking into account the virialization of high overdensities (as in the PS approach) and also the behaviour of very underdense areas (in a way different from the PS prescription). This implies a particular scaling in  $x$  of the counts-in-cells over a well-defined range which is indeed verified by the results of numerical simulations. Thus, our model deals with the evolution of the density field in both linear and non-linear regimes, for any cosmological parameters (open or critical universe) and provides a simple reference to which one could compare the results of a more rigorous treatment. Naturally, our approximation should be tested in more detail with numerical simulations. The density profile of very underdense regions, the evolution with time of the scale and density of typical “voids”, the asymptotic behaviour of the scaling function  $h(x)$ , should allow one to measure the influence of non-spherical corrections and the effects of substructure disruption on the density field, which are not well described by our model, and precise its accuracy.

## References

- Balian R., Schaeffer R., 1989, A&A 220, 1
- Bardeen J.M., Bond J.R., Kaiser N., Szalay A.S., 1986, ApJ 304, 15
- Bernardeau F., 1992, ApJ 392, 1



- Bernardeau F., 1994a, A&A 291, 697  
Bernardeau F., 1994b, ApJ 427, 51  
Bernardeau F., Kofman L., 1995, ApJ 443, 479  
Bernardeau F., Schaeffer R., 1991, A&A 220, 23  
Bernardeau F., van de Weygaert R., Hivon E., Bouchet F.R.,  
1997, MNRAS 290, 566  
Bertschinger E., 1985, ApJS 58,1  
Bond J.R., Cole S., Efstathiou G., Kaiser N., 1991, ApJ 379,  
440  
Bond J.R., Kofman L., Pogosyan D., 1996, Nature 380, 603  
Bouchet F.R., Schaeffer R., Davis M., 1991, ApJ 383, 19  
Cole J., 1951, Quart. Appl. Math. 9, 225  
Cole S., 1989, PhD Thesis  
Cole S., Lacey C.G., 1996, MNRAS 281, 716  
Cole S., Weinberg D.H., Frenk C.S., Ratra B., 1997, MNRAS  
289, 37  
Colombi S., Bouchet F.R., Schaeffer R., 1995, ApJS 96, 401  
Colombi S., Bernardeau F., Bouchet F.R., Hernquist L., 1997,  
MNRAS 287, 241  
Davis M., Efstathiou G., Frenk C., White S.D.M., 1985, ApJ  
292, 371  
Efstathiou G., Frenk C.S., White S.D.M., Davis M., 1988, MN-  
RAS 235, 715  
Ghigna S., Moore B., Governato F., Lake G., Quinn T., Stadel  
J., 1998, submitted to MNRAS, astro-ph 9801192  
Hopf E., 1950, Comm. Pure Appl. Mech. 3, 201  
Kauffmann G., White S.D.M., 1993, MNRAS 261, 921  
Klypin A.A., Gottlober S., Kravtsov A.V., 1998, submitted to  
ApJ, astro-ph 9708191  
Lacey C., Cole S., 1994, MNRAS 271, 676  
Lin C.C., Mestel L., Shu F.H., 1965, ApJ 142, 1431  
Maurogordato S., Schaeffer R., da Costa L.N., 1992, ApJ 390,  
17  
Moore B., Governato F., Quinn T., Stadel J., Lake G., 1998a,  
accepted by ApJL, astro-ph 9709051  
Munshi D., Bernardeau F., Melott A.L., Schaeffer R., 1998,  
submitted to MNRAS, astro-ph 9707009  
Navarro J.F., Frenk C.S., White S.D.M., 1996, ApJ 462, 563  
Navarro J.F., Frenk C.S., White S.D.M., 1997, ApJ 490, 493  
Peacock J.A., Heavens A.F., 1990, MNRAS 243, 133  
Peebles P.J.E., 1980, The Large Scale Structure of the Uni-  
verse, Princeton University Press  
Peebles P.J.E., 1982, ApJL 263, L1  
Press W., Schechter P., 1974, ApJ 187, 425  
Protogeros Z.A.M., Scherrer R.J., 1997, MNRAS 284, 425  
Protogeros Z.A.M., Melott A.L., Scherrer R.J., 1997, MNRAS  
290, 367  
She Z., Aurell E., Frisch U., 1992, Comm. Math. Phys. 148,  
623  
Sinai Y., 1992, Comm. Math. Phys. 148, 601  
Tormen G., Bouchet F.R., White S.D.M., 1997, MNRAS 286,  
865  
Valageas P., Schaeffer R., 1997, A&A 328, 435 (VS)  
Vergassola M., Dubrulle B., Frisch U., Noullez A., 1994, A&A  
289, 325  
Weinberg D.H., Hernquist L., Katz N., Miralda-Escude J.,  
1996, in Cold Gas at High Redshift, ed. M.N. Bremer,  
P.P. van der Werf, H.J.A. Rottgering, C.L. Carilli, (Dor-  
drecht:Kluwer), 93